Supporting Information

Wanigasekera et al. 10.1073/pnas.1120201109

SI Methods

General details of study methods of this experiment have already been published (1). A brief outline of general methods and a detailed account of the methods specific to the data presented in this manuscript are given below. Experimental design is outlined in Fig. S1.

Subjects. The Oxfordshire research ethics committee approved the study and subjects gave written informed consent. Thirty-three healthy subjects (American Society of Anesthesiologists physical status I) were recruited. Of these, 25 subjects (mean age, 30 y; age range, 21–46 y; 11 females) completed the study. Seven subjects were excluded during the screening visit, which was performed to ensure that the subjects tolerated an i.v. infusion of remifentanil (short acting μ-opioid agonist) and the study procedures. One subject failed to attend the subsequent scanning visits.

Study Design and Drug Infusion. For the two scanning visits, subjects received an infusion of remifentanil during one of the visits and a saline infusion during the other (balanced for order), separated by at least 1 wk. The subjects were blinded to the treatment. They fasted for 6 h before commencing the i.v. infusion. Remifentanil was delivered via an indwelling i.v. cannula inserted into the left forearm using a target controlled infusion (TCI) pump to achieve a steady state effect site concentration of 2 ng mL^{-1} for 30 min (2). We used a TCI pump to achieve an equivalent effect site concentration in all subjects during the steady state irrespective of subject demographics. The TCI pump achieves this by selecting the appropriate infusion rate based on the subject demographics to reach the set target effect site concentration. In this way, we minimize the influence of subject demographics on the remifentanil-induced effects (Fig. S4) by delivering a consistent effect site concentration (in this instance, 2 ng/mL) in all subjects during the steady state irrespective of subject demographics.

Total duration of the infusion was 40 min, allowing 10 min to reach the steady-state effect site concentration. Infusion was connected and monitoring was commenced after placing the subject in the scanner. To ensure subject safety throughout the experiment, we monitored the pulse rate, blood oxygen saturation (SpO2), respiratory rate, and end-tidal carbon dioxide partial pressures ($P_{ET}CO_2$) via nasal cannulae (Salter Labs). Oxygen 1–2 L/min was delivered via the nasal cannulae.

We delivered noxious stimuli while obtaining functional scans, assessed the mood levels, and gathered physiological data before (preinfusion period), during, and after the infusion. We used heat and punctate noxious stimuli. These were delivered separately in blocks of 10 stimuli before, during, and after the infusion with the heat stimulation blocks preceding the punctate stimulation blocks.

The data from the postinfusion period and noxious punctate stimuli were used to investigate opioid withdrawal-induced hyperalgesia and are published elsewhere (1).

Noxious Heat Stimulation. The heat stimuli were delivered using an in-house developed thermal resistor with a fast rise time (30° rise in 0.8 s) to deliver noxious heat stimuli via a thermode (3) attached to the medial–volar aspect of the proximal right forearm. The temperature delivered was selected for each subject for each visit with the subject in the scanner but before starting the experiment. By adjusting the temperature of the thermode, we identified a temperature that delivered a noxious stimulus that the subject perceived as moderately painful [5 on a numerical rating scale (NRS) where 0 corresponds to "no pain" and 10 to "severe pain"]. The same temperature was used for all heat stimuli during that visit for the individual volunteer. Ten such stimuli (each lasting for 3 s) were delivered 55–68 s apart before, during, and after the infusion. The intensity of each stimulus as experienced at the time of the noxious stimulus was recorded ∼15 s after the stimulus using a visual analog scale (VAS) displayed on a computer screen where the anchors were "no pain" and "severe pain."

Mood Scale. We tracked the level of tranquility, sociability, mental sedation, and physical sedation using the 16-item Bond-Lader mood scale (4). These were recorded during the preinfusion period, during the infusion period, and during the withdrawal period (∼20 min after stopping the infusion). The mood during the infusion was measured on reaching steady state just before starting the noxious stimulation block and at the end of the stimulation block just before stopping the infusion. The mood during the infusion was considered as the average of these two measurements.

Assessment of Reward Responsiveness Personality Trait. We used Carver and White's behavioral inhibition system (BIS)/behavioral activation system (BAS) scale (5), which characterizes individual personalities in terms of their response to aversive and rewarding stimuli. The BIS scale consists of items referencing to a punishing event. The BAS scale has three subscales: reward responsiveness (RWR), drive, and fun seeking. These have items focusing on positive responses to the experience or anticipation of a reward (RWR), relating to persistent pursuit of desired goals (drive), and reflecting the desire for new rewards and a willingness to approach a potentially rewarding event impulsively (fun seeking). These personality traits are underpinned by endogenous neurotransmitters such as dopamine (6), norepinephrine (7), serotonin (8), and opioids (9). The subscales used in these studies are from Cloniger's tridimentional personality questionnaire that has been validated against the BIS/BAS scale. Although these neurotransmitter systems interact with each other, we felt that it is important to assess the subscales differently as they measure different aspects of the behavioral activation system. This also makes the total BAS scale inappropriate to study a specific aspect of the behavioral activation system. Because we were examining an individual's response to a reward, in this instance, opioid-induced analgesia, we used the RWR subscale.

The subjects completed this questionnaire during the first scanning visit before any study intervention.

fMRI Data Acquisition. Functional imaging data were acquired using a 3T Varian-Siemens whole-body magnetic resonance scanner. We used a head-only gradient coil with a birdcage radiofrequency coil for pulse transmission and signal reception. A whole-brain (including the midbrain, pons, rostralmost medulla, and cerebellum) T2*-sensitive gradient echo-planar imaging (EPI) sequence with the following parameters was used: 3-s repetition time (TR), 30-ms echo time (TE), 0.5494-ms dwell time, 42 contiguous 3.5-mm-thick slices, field of view (FOV) 224 × 224 mm, and matrix 64 × 64. Functional scans acquired during the heat stimulation block consisted of 210 volumes. The first four volumes were discarded to permit equilibration of the blood oxygen level dependent (BOLD) signal. Fieldmaps were obtained using a symmetric-asymmetric spin-echo sequence after the preinfusion period functional scans. A T1 weighted structural (1 mm^3 voxel) image was acquired for the registration of statistical activation maps to the standard stereotactic space [Montreal Neurological Institute (MNI), 152 template].

Analysis of Psychophysical Data. Twenty-three complete datasets were available for analysis. D'Agostino and Pearson's omnibus normality test was used to examine the distribution of psychophysical data. For normally distributed data, the paired two-tailed t test was used for comparison of preinfusion period data from the two visits. A one-sample two-tailed t test was performed to evaluate whether the distribution of the opioid infusion-induced effects were significantly different from a mean of zero. For data that were nonnormally distributed, we used the Wilcoxon signed rank test.

Detection of differences in preinfusion period data. We tested for significant differences between the two visits in the following preinfusion period data: temperatures used, noxious stimulus intensity, the four aspects of the mood scale, and the four cardiorespiratory variables.

Detection of opioid-induced changes in psychophysical data. The opioid infusion induced effect for a given set of psychophysical variables (v) was defined by [v opioid$_{(\text{infusion}-\text{preinfusion})}$] − [$v$ saline$_{(\text{infusion}-\text{preinfusion})}$]. Subtracting the preinfusion period values from the infusion period values accounts for any preinfusion period differences between the visits. Subtracting the differences in the saline visit from those in the opioid visit accounts for the effect of time.

A negative value for an opioid infusion-induced effect indicates a reduction, whereas a positive value indicates an increase. To depict opioid-induced behavioral analgesia as a positive value, we defined it as [v opioid$_{(\text{preinfusion}-\text{infusion})}$] − [$v$ saline$_{(\text{basleine}-\text{infusion})}$], where v is pain intensity.

Correlation analysis. To test our hypothesis, we performed a correlation analysis between the trait reward responsiveness and the opioid-induced analgesia. We also performed a correlation analysis between opioid-induced behavioral analgesia and the opioid-induced mood changes. We assessed this relationship because mood and pain are known to influence each other (10). Furthermore, opioids not only result in analgesia but also in mood changes.

As we had a perception-matched stimulus for each subject during each visit, a change in nociceptive input between sessions and between subjects potentially can occur. Therefore, to assess the influence of temperature used on behavioral opioid analgesia, we performed a correlation analysis between these two parameters.

To confirm that we had minimized the influence of subject demographics on the remifentanil-induced behavioral analgesia by using a TCI pump to deliver the remifentanil, we performed correlation analyses between the analgesia score and subject demographics.

Analysis of fMRI Data. fMRI analyses were performed using FEAT (FMRI Expert Analysis Tool) version 5.98, part of the Oxford Centre for Functional Magnetic Resonance Imaging of the Brain software library (FSL); www.fmrib.ox.ac.uk/fsl. Preprocessing steps included motion correction (11), field-map correction of EPI distortion (12), removal of nonbrain voxels (13), spatial smoothing using a Gaussian kernel of the full width at half maximum 5-mm grand-mean intensity normalization of the entire 4D dataset by a single multiplicative factor and highpass temporal filtering with a cutoff of 100 s. Time-series statistical analysis was performed with local autocorrelation correction (14).

First-level analysis. Statistical analysis was performed for each of the functional scans for individual subjects using a general linear modeling approach. The input stimulus functions defined for the noxious stimuli and the rating tasks were convolved with the gamma hemodynamic function (mean lag, 6 s; full width at half height, 6 s) to yield regressors for the general linear model that described the BOLD activity in the functional scans. The estimated motion parameters for each subject were included as nuisance regressors. These analyses generated the parameter estimates (PEs) for the regressors that described the BOLD activity evoked by noxious stimuli for each stimulation block. Registration of functional images to each subject's high resolution T_1 scan, and then to the MNI standard brain was carried out using FLIRT (15).

Higher-level analysis. For all voxelwise brain analyses, we used mixed effects analysis (16) and a cluster-based correction for familywise error rate (FWR) (Z score >2.3; FWR $P < 0.05$). For hypothesis-driven searches, we performed a small volume correction using nonparametric permutation testing (5,000 permutations) (17) and threshold free cluster enhanced (TFCE) FWR correction at $P < 0.05$ (18). For small volume corrections (directed searches), regions were defined using the Harvard Oxford Cortical and Subcortical Structural Atlas (http://www.fmrib.ox.ac.uk/fsl/data/atlas-descriptions.html), which is a probabilistic population-based atlas. Only voxels estimated at greater than 50% probability of being in the structure were included in the region. For defining correct identification of brainstem areas, we used the Duvernoy Brainstem Atlas (19) because an automated detailed brainstem atlas is not available.

We used Featquery (http://fsl.fmrib.ox.ac.uk/fsl/fslwiki/FEAT/UserGuide#Featquery_output) for extraction of percentage of BOLD signal change evoked by the task from the significantly active voxels within an anatomical area. When extracting data from the brainstem structures, we used the Duvernoy Brainstem Atlas for correct identification of anatomical areas in the brainstem.

Using a voxelwise brain analysis and a paired test, we first searched for differences in brain activity evoked by noxious stimuli in the preinfusion periods between the two visits for the whole group.

Identifying areas of the brain where the preinfusion period neuronal response to noxious stimuli predicts the magnitude of opioid behavioral analgesia. The two preinfusion period statistical maps of each subject generated at the first-level analysis were entered into a second-level analysis with fixed effects to produce a statistical map that represented the average neuronal response to noxious stimuli during the preinfusion period for an individual subject. Using these maps, we next performed a voxelwise brain analysis (mixed effects analysis and a cluster-based correction for multiple comparisons: Z score >2.3; FWR $P < 0.05$) at the third level using a model containing a regressor for the group mean and another regressor with the opioid-induced behavioral analgesia score.

We also performed small volume corrections (nonparametric permutation testing and TFCE FWR correction at $P < 0.05$) to examine this relationship using nine directed searches in the key reward processing areas of the brain namely the bilateral nucleus accumbens (NAc), caudate, amygdala, hippocampus, and the mesencephalic tegmentum. (See Fig. S5 for the masks used.) The mesencephalic tegmentum was used for searching for activity in the ventral tegmental area (VTA). In this mask we included the area of the mesencephalon between a line drawn ventral to the aqueduct separating the tectum from the tegmentum, and a line drawn ventral to the substantia nigra separating the tegmentum from the white matter tracts.

To illustrate any significant relationships identified by these image analyses we extracted the percentage of BOLD signal response from the voxels in relevant areas. We then plotted these against the opioid-induced behavioral analgesia score.

To examine the relationship between the preinfusion period percentage of BOLD signal response to noxious stimuli from these voxels and the reward responsiveness score we performed a correlation analysis (Pearson's r) between these two variables.

Identifying areas with opioid-induced changes in neuronal response to noxious stimuli. For each subject, in a second level analysis using fixed effects we generated a statistical map representing the opioid infusion-induced changes in the neuronal response to noxious stimuli. For this analysis we used the outputs generated by the first-level analyses from the functional scans of the two preinfusion periods and the two infusion periods. We defined the opioid-induced changes in the neuronal response to noxious stimuli as

$[v\ \text{opioid}_{(\text{preinfusion}-\text{infusion})}] - [v\ \text{saline}_{(\text{preinfusion}-\text{infusion})}]$, where v is the BOLD response evoked by noxious stimuli. A positive value indicates the magnitude of the opioid-induced reduction of the neuronal response to noxious stimuli. This is the same method used for defining opioid-induced behavioral analgeisa as described previously.

Using these maps, we next performed a voxelwise analysis (mixed effects analysis and a cluster-based correction for multiple comparisons; Z score >2.3, FWR $P < 0.05$) at the third level using a model containing a regressor for the group mean of the opioid-induced changes in the neuronal response to noxious stimuli and another regressor with the opioid-induced behavioral analgesia score.

This would specifically identify areas of the brain with opioid-induced changes in neuronal response to noxious stimuli that correlated with the magnitude of the behavioral analgesia score. These would be areas of the brain that are implicated in mediating opioid-induced behavioral analgesia including the structures of the descending pain modulatory system (DPMS).

We used a small volume correction (nonparametric permutation testing and TFCE FWR correction at $P < 0.05$) to study this relationship in areas of the reward circuitry where the neuronal response to noxious stimuli during the preinfusion period predicted the magnitude of opioid-induced analgesia. These were the rostral anterior cingulate cortex (rACC), left orbitofrontal cortex (OFC), right and left amygdala, right and left hippocampus, right accumbens, left caudate, and the mesencephalic tegmentum. Clearly if these structures/areas predicted the behavioral analgesia at baseline, then there is a strong possibility that they could play a role in the opioid-induced response (masks shown in Fig. S5). The masks of the rACC area and left OFC are from the cluster of voxels with preinfusion period brain activity that significantly predicted behavioral analgesia. We used this method because the rACC is not defined in standard atlases and the OFC is a large area with functional diversity (20).

To illustrate any significant relationships identified by these image analyses we extracted the percentage of BOLD response from the voxels in relevant areas. Then we derived the opioid-induced change in percentage of BOLD response and plotted it against the opioid-induced behavioral analgesia score.

To examine the relationship between the opioid-induced changes in percentage of BOLD response to noxious stimuli from these voxels (voxels that showed a significant relationship in the above image analyses) and the reward responsiveness score we performed a correlation analysis (Pearson's r) between these two variables.

To examine the role of the key nuclei in the reward circuitry with preinfusion period brain activity that predicted subsequent behavioral analgesia, namely, the right NAc and the VTA, we performed another analysis. For this we used the group mean maps of the opioid-induced changes in brain activity and a regressor for the neuronal (extracted percentage of BOLD) response to noxious stimuli during the preinfusion period from the voxels in the right NAc and VTA (key nuclei in the reward circuitry) that predicted the behavioral analgesia score. For this analysis we limited the search to bilateral amygdala, left hippocampus, periaqueductal gray (PAG), and rostral ventromedial medulla (RVM), as they contributed to the expression of opioid analgesia in our study and are components of the DPMS as well as reward circuitry (masks shown in Fig. S5).

SI Results

Of the 33 subjects recruited, 25 (mean age, 30 y; age range, 21–46 y; 11 females) completed a two-way crossover study. Of the eight subjects not scanned, five were excluded due to opioid-induced nausea during the screening visit, one subject was intolerant of the i.v. cannula, one subject was claustrophobic in the scanner, and one subject failed to attend both scanner sessions.

Datasets from 23 of the 25 subjects were analyzed. Data from one subject was excluded because the average threshold temperature of 41 °C was well below the nociceptive threshold and more than two SDs lower than the rest of the subjects. The data from the other subject were excluded due to motion artifacts and incorrect timing in the functional scans due to equipment malfunction.

Preinfusion Period: Psychophysical Data. There are no significant differences ($P > 0.05$) in group means of the following preinfusion period psychophysical variables between the two visits: temperature required to elicit moderately painful stimuli, perceived intensity of the heat noxious stimulus, mood (tranquility, sociability, mental sedation, and physical sedation), or cardiorespiratory variables [end-tidal carbon dioxide partial pressures ($P_{ET}CO_2$), respiratory rate, blood oxygen saturation (SpO2), and pulse rate].

Group mean value (±SD) of these preinfusion period variables during the saline visit for the temperature used was 50.8 °C (±1.7), heat pain intensity (visual analog scale, VAS) was 5.1 (±0.8), tranquility (VAS) was 7.5 (±1.5), sociability (VAS) was 7.0 (±1.4), mental sedation (VAS) was 3.1 (±1.8), physical sedation (VAS) was 2.9 (±1.3), $P_{ET}CO_2$ (in millimeters of mercury) was 41.2 (±4.3), respiratory rate (breaths per minute) was 15 (±3), SpO2 (percentage) was 98.4 (±0.8), and pulse rate (beats per minute) was 58 (±7).

Group mean value (±SD) of these preinfusion period variables during the remifentanil visit for the temperature used was 50.6 °C (±1.9), heat pain intensity (VAS) was 5.1 (±1.0), tranquility (VAS) was 7.5 (±1.6), sociability (VAS) was 7.1 (±1.5), mental sedation (VAS) was 2.9 (±2.1), physical sedation (VAS) was 2.8 (±1.6), $P_{ET}CO_2$ (in millimeters of mercury) was 40.6 (±4.0), respiratory rate (breaths per minute) was 15 (±3), SpO2 (%) was 98.7 (±0.7), and pulse rate (beats per minute) was 58 (±8).

Preinfusion Period: fMRI Data. There are no significant differences in the neuronal response to noxious stimuli between the remifentanil and saline preinfusion periods anywhere in the brain. This is consistent with preinfusion period psychophysical data that show no differences between the two visits.

There is a positive correlation between the preinfusion period brain activity (extracted percentage of BOLD) from voxels in reward regions that predicted behavioral analgesia and subjects' trait reward responsiveness (RWR) scores. This relationship is statistically significant in the following areas: left OFC ($r = 0.5$; $P = 0.01$), rACC ($r = 0.44$; $P = 0.04$), right accumbens ($r = 0.54$; $P = 0.01$); left caudate ($r = 0.46$; $P = 0.03$); right amygdala ($r = 0.42$; $P = 0.045$); left amygdala ($r = 0.55$; $P = 0.01$), and right hippocampus ($r = 0.44$; $P = 0.04$). This relationship in the VTA ($r = 0.37$; $P = 0.08$) and left hippocampus ($r = 0.32$; $P = 0.13$) failed to reach statistical significance.

Opioid-Induced Changes: Psychophysical Data. Remifentanil at an effect site concentration of 2 ng mL^{-1} induced the following mood changes: significant increases ($P < 0.01$) in mental and physical sedation and nonsignificant increases in tranquility and sociability (Fig. S2). These opioid-induced changes do not show a significant correlation with either the opioid-induced behavioral analgesia or the RWR trait ($P \geq 0.16$).

There were no significant influences of temperature used nor subject demographics on behavioral opioid-induced analgesia (Fig. S4).

As anticipated the opioid infusion induces a statistically significant reduction in the respiratory rate ($P < 0.01$), a higher $P_{ET}CO_2$ ($P < 0.01$) and a reduction in SpO_2 ($P < 0.05$). The mean changes (±SD) for respiratory rate is 3.7 (±3) breaths/min, $P_{ET}CO_2$ is 5.5 (±4.2) mmHg, and SpO_2 is 0.5 (±0.8) %. These changes are clinically insignificant and did not compromise

the safety of the subject. There are no significant opioid-induced changes in the pulse rate.

Opioid-Induced Changes: fMRI Data. The opioid-induced changes in neuronal (extracted percentage of BOLD) response to noxious stimuli in voxels that showed a significant correlation with the magnitude of the behavioral opioid analgesia failed to show a significant correlation with trait RWR. The correlation coefficient of this relationship in the thalami is 0.33 ($P = 0.13$), in PAG, 0.03 ($P = 0.89$), in RVM, 0.28 ($P = 0.20$), in left hippocampus, 0.35 ($P = 0.10$), in right amygdala, 0.33 ($P = 0.12$), and in left amygdala, 0.37 ($P = 0.10$).

1. Wanigasekera V, Lee MC, Rogers R, Hu P, Tracey I (2011) Neural correlates of an injury-free model of central sensitization induced by opioid withdrawal in humans. *J Neurosci* 31:2835–2842.
2. Minto CF, Schnider TW, Shafer SL (1997) Pharmacokinetics and pharmacodynamics of remifentanil. II. Model application. *Anesthesiology* 86:24–33.
3. Wise RG, et al. (2002) Combining fMRI with a pharmacokinetic model to determine which brain areas activated by painful stimulation are specifically modulated by remifentanil. *Neuroimage* 16:999–1014.
4. Bond AJ, James DC, Lader MH (1974) Physiological and psychological measures in anxious patients. *Psychol Med* 4:364–373.
5. Carver C (1994) Behavioral inhibition, behavioral activation, and affective responses to impending reward and punishment: The BIS/BAS scale. *J Pers Soc Psychol* 67: 319–333.
6. Zald DH, et al. (2008) Midbrain dopamine receptor availability is inversely associated with novelty-seeking traits in humans. *J Neurosci* 28:14372–14378.
7. Garvey MJ, Noyes R, Jr., Cook B, Blum N (1996) Preliminary confirmation of the proposed link between reward-dependence traits and norepinephrine. *Psychiatry Res* 65:61–64.
8. Hansenne M, Ansseau M (1999) Harm avoidance and serotonin. *Biol Psychol* 51:77–81.
9. Schreckenberger M, et al. (2008) Opioid receptor PET reveals the psychobiologic correlates of reward processing. *J Nucl Med* 49:1257–1261.
10. Villemure C, Bushnell MC (2009) Mood influences supraspinal pain processing separately from attention. *J Neurosci* 29:705–715.
11. Jenkinson M, Bannister P, Brady M, Smith S (2002) Improved optimization for the robust and accurate linear registration and motion correction of brain images. *Neuroimage* 17:825–841.
12. Jenkinson M (2003) Fast, automated, N-dimensional phase-unwrapping algorithm. *Magn Reson Med* 49:193–197.
13. Smith SM (2002) Fast robust automated brain extraction. *Hum Brain Mapp* 17: 143–155.
14. Woolrich MW, Ripley BD, Brady M, Smith SM (2001) Temporal autocorrelation in univariate linear modeling of FMRI data. *Neuroimage* 14:1370–1386.
15. Jenkinson M, Smith S (2001) A global optimisation method for robust affine registration of brain images. *Med Image Anal* 5:143–156.
16. Woolrich MW, Behrens TE, Beckmann CF, Jenkinson M, Smith SM (2004) Multilevel linear modelling for FMRI group analysis using Bayesian inference. *Neuroimage* 21: 1732–1747.
17. Nichols TE, Holmes AP (2002) Nonparametric permutation tests for functional neuroimaging: A primer with examples. *Hum Brain Mapp* 15:1–25.
18. Smith SM, Nichols TE (2009) Threshold-free cluster enhancement: Addressing problems of smoothing, threshold dependence and localisation in cluster inference. *Neuroimage* 44:83–98.
19. Naidich TP, et al. (2009) *Duvernoy's Atlas of the Human Brain Stem and Cerebellum* (Springer, New York).
20. O'Doherty JP (2007) Lights, camembert, action! The role of human orbitofrontal cortex in encoding stimuli, rewards, and choices. *Ann N Y Acad Sci* 1121:254–272.

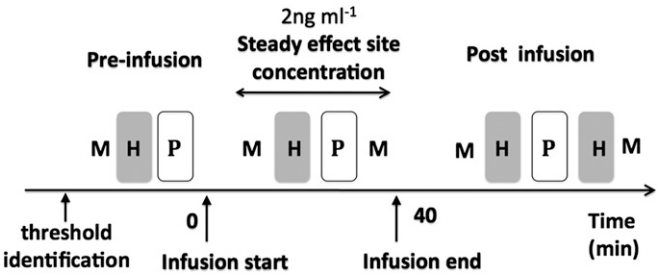

Fig. S1. Experimental paradigm. After identifying the threshold, heat stimulation (H) was performed before, during, and after infusion. Punctate stimulation (P) was performed after every heat stimulation block. Functional scans were performed during noxious stimulation blocks. Mood (M) was assessed before infusing the drug, twice during the infusion, and twice during the postinfusion period. Remifentanil steady-effect site concentration of 2 ng mL^{-1} was maintained for 30 min. Total duration of the infusion was 40 min. Punctate stimuli and all of the measurements after the infusion were for the purpose of investigating opioid-induced hyperalgesia (published elsewhere).

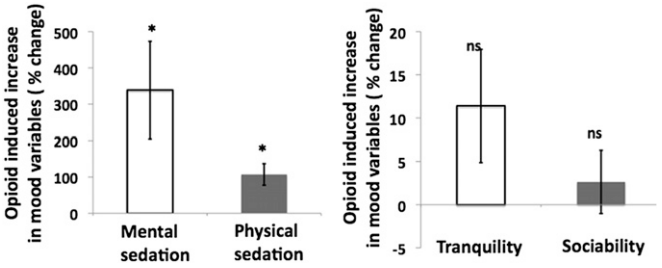

Fig. S2. Opioid-induced increases in mood variables. The *y* axis (*Left* graph) shows the mean opioid-induced increase (as percentage of change) in mental (open bar) and physical (black bar) sedation. The *y* axis (*Right* graph) shows the mean opioid-induced increase (as percentage of change) in tranquility (open bar) and sociability (black bar). Error bars indicate SEM. *$P < 0.01$; NS, not significant ($P > 0.05$). The opioid-induced increase in mood is defined as $[v\ \text{opioid}_{(\text{infusion} - \text{preinfusion})}] - [v\ \text{saline}_{(\text{infusion} - \text{preinfusion})}]$, where v is the mood variable.

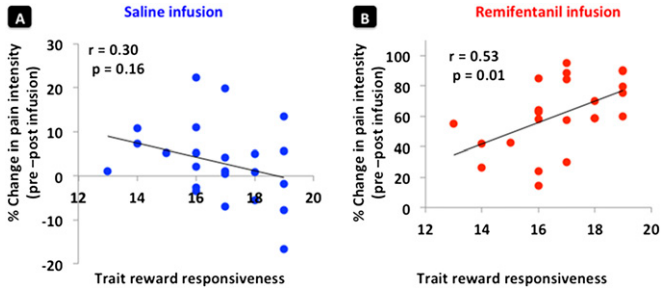

Fig. S3. Relationship between the trait reward responsiveness and changes in pain intensity during the saline (*A*) and remifentanil (*B*) infusions. The *y* axis shows the mean percentage change in pain intensity of noxious heat stimuli from the preinfusion period during each infusion. Trait reward responsiveness (RWR) scores are in the *x* axis. There is a significant positive correlation ($r = 0.53$; $P = 0.01$) between the RWR and the changes in pain intensity induced by the remifentanil infusion. No such relationship is noted during the saline infusion.

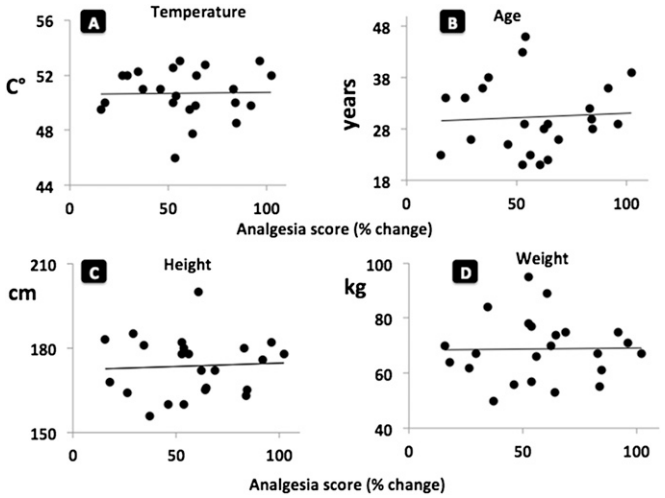

Fig. S4. Absence of influence on opioid-induced analgesia by the temperature used and subject demographics. Analgesia score (percentage of change in pain intensity) in the *x* axis is defined as [*v* opioid$_{(\text{preinfusion} - \text{infusion})}$] − [*v* saline$_{(\text{preinfusion} - \text{infusion})}$], where *v* is pain intensity. (*A*) *Y* axis, temperature used; (*B*) *y* axis, age of the subjects; (*C*) *y* axis, height of the subjects; (*D*) *y* axis, weight of the subjects.

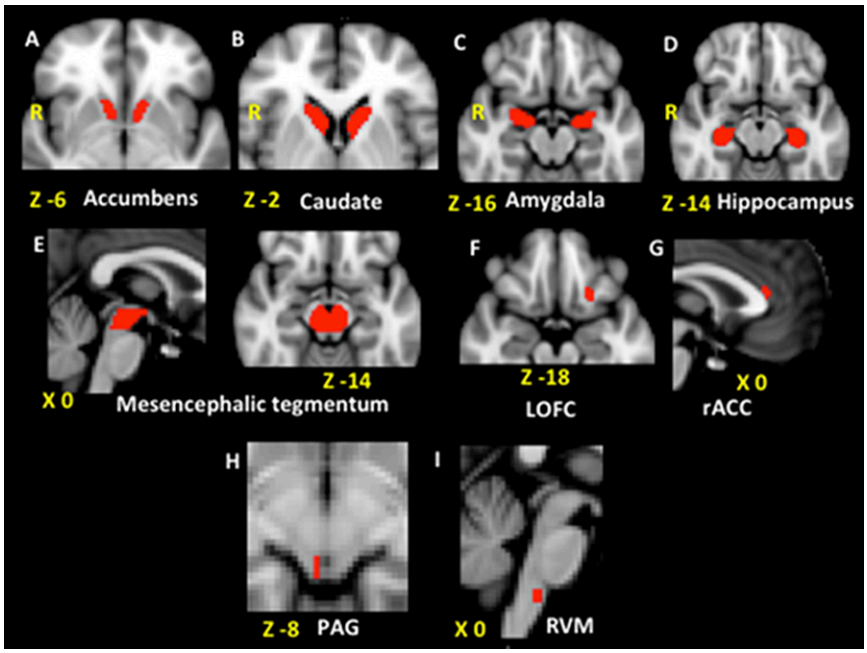

Fig. S5. Masks of the a priori regions of the reward network used for directed searches. Masks are overlaid on a standard structural image. Montreal Neurological Institute (MNI) coordinates are denoted in millimeters below each slice. Masks used for identifying preinfusion period neuronal response to noxious stimuli that predict opioid-induced behavioral analgesia were: right and left nucleus accumbens (*A*), right and left caudate (*B*), right and left amygdala (*C*), right and left hippocampus (*D*), and the mesencephalic tegmentum (*E*). Masks used for identifying areas of the brain where there is a significant positive correlation between the opioid-induced changes in neuronal response to noxious stimuli and opioid-induced behavioral analgesia were: an area of the left orbitofrontal cortex (LOFC) (*F*), an area of rostral anterior cingulate cortex (rACC) (*G*), right and left amygdala (*C*), right and left hippocampus (*D*), right accumbens (*A*), left caudate (*B*), and the mesencephalic tegmentum (*E*). Masks used for identifying areas where there is a significant positive correlation between the preinfusion period neuronal response to noxious stimuli in the ventral tegmental area (VTA) and opioid-induced changes in neuronal response to noxious stimuli were: the left hippocampus (*D*), bilateral amygdala (*C*), an area in the periaqueductal gray (PAG) (*H*), and an area in the rostral ventromedial medulla (RVM) (*I*).

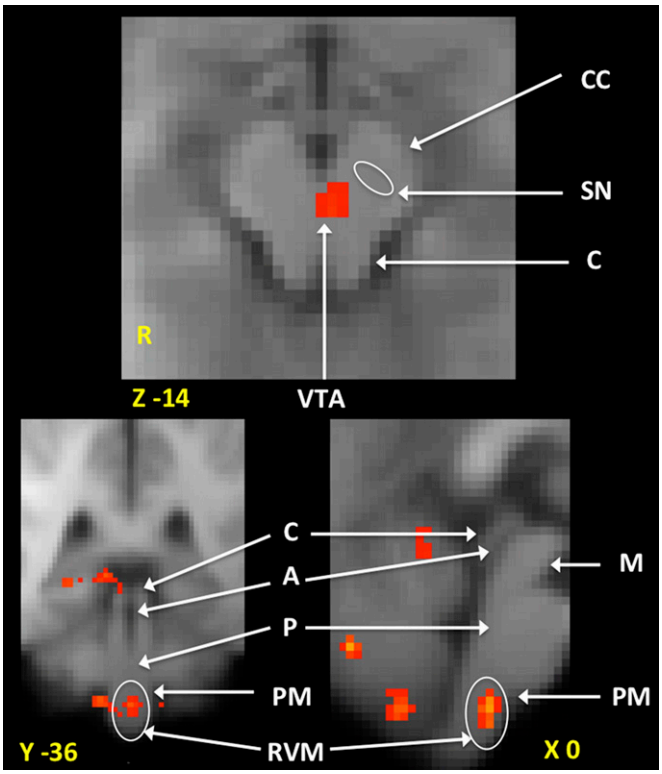

Fig. S6. Localization of the cluster of voxels in the midbrain ventral tegmental area (VTA) and the cluster of voxels in the rostral ventromedial medulla (RVM). The activity is displayed on the group average structural image. Montreal Neurological Institute (MNI) coordinate is indicated in millimeters below the image slices. The cluster of voxels in the VTA (*Upper* image) is where the preinfusion period neuronal response to noxious stimuli predicted opioid-induced behavioral analgesia. See Duvernoy's atlas of the human brainstem and cerebellum (19) to aid identification of anatomical areas. C, colliculi; SN, substantia nigra; CC, crus cerebri. The cluster of voxels in the RVM (*Lower* images) is where opioid-induced changes in neuronal response to noxious stimuli show a significant positive correlation with opioid-induced behavioral analgesia. The activity we observed is in the most rostral and medial aspect of the medulla at the pontomedullary junction as shown by the sagittal image slice on the right and the coronal image slice on the left. The medial and ventral aspects of the rostral medulla in this area contain the nucleus raphe pallidus and the nucleus reticularis gigantocellularis. The image resolution in our results is insufficient to make any claims on activity in specific RVM nuclei. See Duvernoy's atlas of the human brainstem and cerebellum (19) to aid identification of anatomical areas. C, colliculi; A, aqueduct; P, pons in the floor of the IVth ventricle; PM, pontomedullary junction; M, mesencephalon.

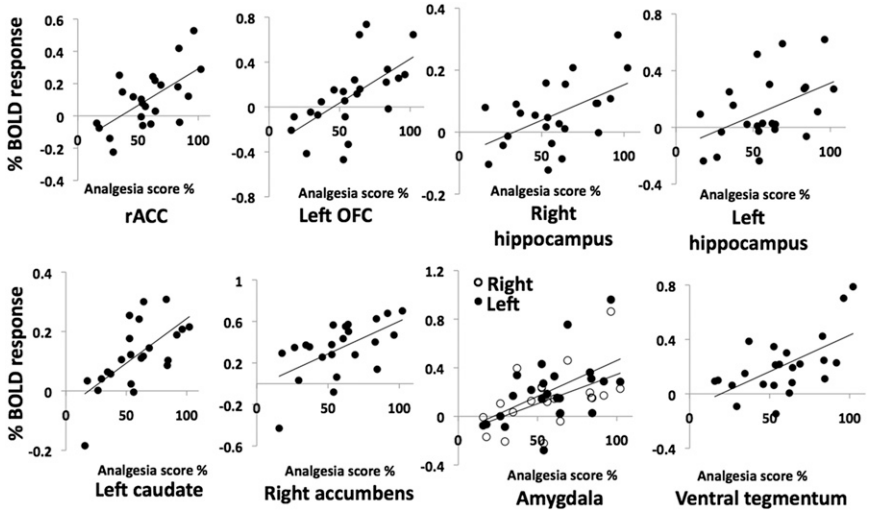

Fig. S7. Scatter plots illustrating the preinfusion period neuronal response to noxious stimuli predicting behavioral analgesia. Preinfusion period neuronal response as percentage of BOLD signal is on the *y* axis. Analgesia score as percentage of change in pain intensity is on the *x* axis. Opioid-induced behavioral analgesia is defined as $[v\ \text{opioid}_{(\text{preinfusion} - \text{infusion})}] - [v\ \text{saline}_{(\text{preinfusion} - \text{infusion})}]$, where *v* is the pain intensity. Percentage of BOLD responses are from the clusters of voxels in areas of the rostral anterior cingulate cortex (rACC), left orbitofrontal cortex, right and left hippocampus (*Upper* row from *Left* to *Right*), the left caudate, right nucleus accumbens, bilateral amygdala (right amygdala in open circles), and the ventral tegmentum (*Lower* row, *Left* to *Right*).

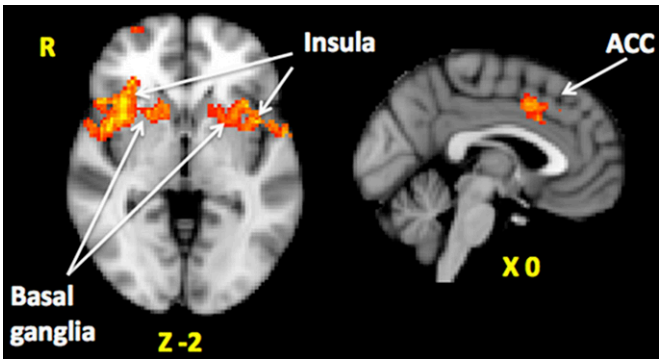

Fig. S8. Areas of the brain with significant opioid-induced reduction in neuronal response to noxious stimuli. Clusters of voxels in areas of the anterior cingulate cortex (ACC), bilateral basal ganglia (putamen and caudate), and insula are shown. Image slices are from the mean statistical map representing significant opioid-induced reductions in neuronal response to noxious stimuli (cluster-based correction: Z score >2.3; $P < 0.05$). Opioid-induced neuronal response is defined as [v opioid$_{(\text{preinfusion} - \text{infusion})}$] − [$v$ saline$_{(\text{preinfusion} - \text{infusion})}$], where v is the neuronal response to noxious stimuli. Montreal Neurological Institute coordinates are denoted in millimeters below each slice.

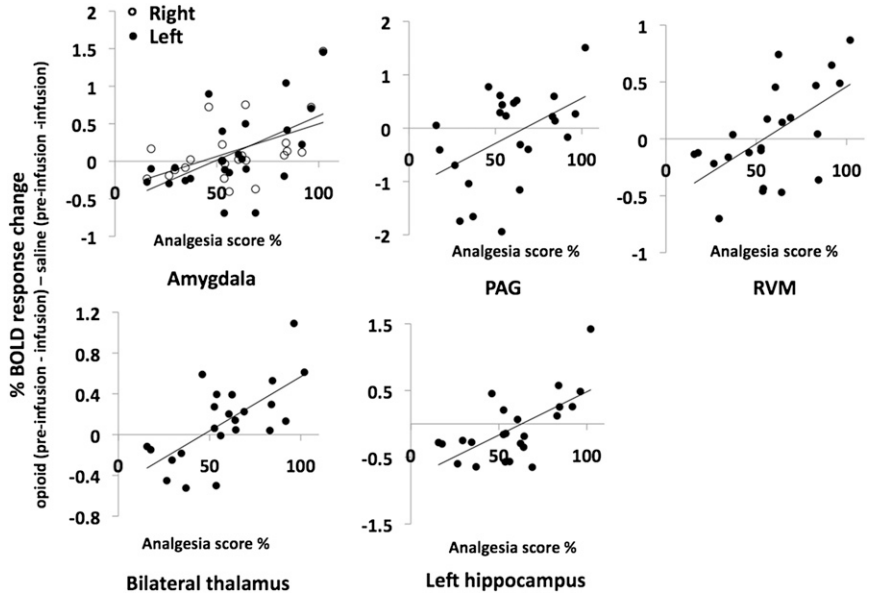

Fig. S9. Scatter plots illustrating the significant positive correlation between opioid-induced behavioral analgesia and opioid-induced changes in neuronal response to noxious stimuli. Opioid-induced changes in neuronal response (percentage of BOLD response) and analgesia (percentage of change in pain intensity) are defined as [v opioid$_{(\text{preinfusion} - \text{infusion})}$] − [$v$ saline$_{(\text{preinfusion} - \text{infusion})}$], where v is the percentage of BOLD response or the pain intensity of noxious stimuli. A positive value for the change in percentage of BOLD response indicates an opioid-induced reduction in the neuronal response. Opioid-induced change in neuronal response as percentage of BOLD response change is on the y axis. Analgesia score as percentage of change in pain intensity is on the x axis. Percentage of BOLD response changes are from the clusters of voxels in areas of the bilateral amygdala (right amygdala in open circles), periaqueductal gray (PAG), rostral ventromedial medulla (RVM) (*Upper* row from *Left* to *Right*), bilateral thalamus, and left hippocampus (*Lower* row, *Left* to *Right*).